A 3-D 160-Site Microelectrode Array for Cochlear Nucleus Mapping

Sister Mary Elizabeth Merriam, Susanne Dehmel, Onnop Srivannavit, Susan E. Shore, and Kensall D. Wise*, *Life Fellow, IEEE*

***Abstract*—A 3-D application-specific microelectrode array has been developed for physiological studies in guinea pig cochlear nucleus (CN). The batch-fabricated silicon probes contain integrated parylene cables and use a boron etch-stop to define 15μm-thick shanks and limit tissue displacement. Targeting the ventral (three probes) and dorsal (two probes) subnuclei, the custom four-shank 32-site probes are combined in a slotted block platform having a 1.18-mm^2 footprint. The device has permitted, for the first time, high-density 3-D *in vivo* studies of ventral CN to dorsal CN connections, stimulating with 1000 μm^2 sites in one subnucleus while recording with 177 μm^2 sites in the other. Through these experiments, it has demonstrated the efficacy of bimodal silicon arrays to better understand the central nervous system at the circuit level. The 160 electrode sites also provide a high-density neural interface, which is an essential aspect of auditory prosthesis prototypes.**

***Index Terms*—Auditory brainstem prosthesis, cochlear nucleus, microelectrode array, neural mapping, silicon probe, 3-D microassembly of microelectromechanical devices.**

I. Introduction

ADVANCES in neuroscience depend on the availability of supporting technology for the high-density stimulation and recording of neural activity. While electrode arrays can be highly versatile, individual neuroscience applications may require particular array specifications for optimal performance [1].

As alternatives to cochlear implants, research on a central auditory prosthesis is targeting the auditory nerve [2], the cochlear nucleus (CN) [3], [4], and the inferior colliculus [5] to lower thresholds, increase dynamic range, and improve frequency discrimination [2], [6]. Placement within the CN may be advantageous since, although, sound coding is divided into parallel channels, the more complex signal-processing functions are left to the higher portions of the auditory system [4]. While research on animal models and clinical trials has shown the potential for such devices, significant technological and neuroscience questions must be addressed before high-quality auditory brainstem implants (ABIs) become a reality. Increasing the number of implanted electrode sites and properly tailoring their 3-D locations to the targeted neural structures is one essential aspect [1], [4]. Once the proper supporting technology exists, the neuroscience experiments needed to determine the sound encoding strategies that will be most successful can be pursued.

The array presented here is an application-specific design with 160 electrode sites to enable the mapping of neural connections between the ventral CN (VCN) and dorsal CN (DCN) in guinea pig [7], [8]. It can also be used as an acute prototype for a central auditory prosthesis.

Manuscript received July 8, 2010; accepted September 13, 2010. Date of publication October 18, 2010; date of current version January 21, 2011. *Asterisk indicates corresponding author*.

M. E. Merriam is with St. Dominic Savio Catholic High School, Austin, TX 78717 USA (e-mail: sisterme@umich.edu).

S. Dehmel is with Kresge Hearing Research Institute, Department of Otolaryngology, University of Michigan, Ann Arbor, MI 48109 USA (e-mail: dehmels@umich.edu).

O. Srivannavit is with of Michigan, Ann Arbor, MI 48109 USA (e-mail: onnops@umich.edu).

S. E. Shore is with the Department of Molecular and Integrative Physiology and the Department of Otolaryngology, University of Michigan, Ann Arbor, MI 48109 USA (e-mail: sushore@umich.edu).

*K. D. Wise Department of Electrical Engineering and Computer Science, University of Michigan, Ann Arbor, MI 48105 USA (e-mail: wise@umich.edu).

Color versions of one or more of the figures in this paper are available online at http://ieeexplore.ieee.org.

Digital Object Identifier 10.1109/TBME.2010.2088122

II. Array Design

A. Anatomical and Surgical Constraints

While the basic anatomical structure of the guinea pig CN and its placement within the brain is well known [9], the numerical details required for a single 3-D array to simultaneously reach the anterio-ventral portion (AVCN) and the DCN are not readily available from current literature. In order to acquire the necessary information for probe and platform specifications, mock arrays with fluorescent fluorogold (FG) dye applied to the shanks were inserted and 3-D reconstructions of serial sections were assembled.

The CN is located in the auditory brainstem. The operative procedure involves removing part of the skull and overlying cerebellum to reach the DCN, as shown in Fig. 1. The access hole is made as small as possible to minimize the surgical impact. While the surgery and cerebellum removal directly exposes the surface of the DCN, the AVCN is located farther ventral, lateral, and rostral. Thus, the VCN shanks pass through the cerebellum to reach the AVCN. The small diameter of the access hole and the angle at which the array must be inserted leads to considerable size and positioning constraints on the electrode array, particularly on the platform and any required cabling. The difference between the mediolateral location of the DCN and the AVCN necessitates offset between the platform positions of the probes designated for the respective regions. The relative dorsoventral and rostrocaudal positions of the CN subdivisions determine the insertion angle and relative probe lengths.

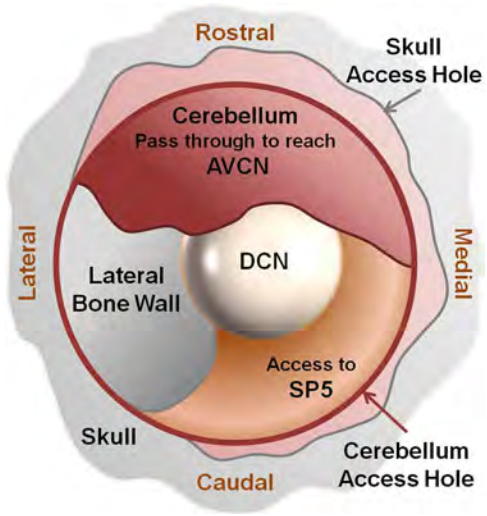

Fig. 1. Conceptual drawing of the surgical region. SP5 = spinal trigeminal nucleus.

TABLE I
SPECIFICATIONS FOR VCN–DCN PROBES

Probe Target Tissue	VCN	DCN
Probe Back-end Major Width	800μm	800μm
Probe Back-end Minor Width	661μm	661μm
Shanks per Probe	4	4
Shank Length[a]	5000μm	3400μm
Shank Length Stagger	0μm	125μm
Shank Pitch	200μm	125μm
Maximum Shank Width	61μm	61μm
Minimum Shank Width	57μm	31μm
Tip to First Site Distance	103μm	50μm
Recording Sites per Shank	4	8
Recording Site Area	177μm^2	177μm^2
Recording Site Pitch	300μm	100μm
Stimulation Sites per Shank	4	n/a
Stimulation Site Area	1000μm^2	n/a
Stimulation Site Pitch	300μm	n/a
Integrated Cable Main Width	692μm	692μ
Integrated Cable Length	10mm	10mm

[a]Shank length is measured from the bottom of the platform to the center of the tip-most site on the longest shank.

B. 2-D VCN–DCN Probes for Use in the 3-D Array

For a high-density interface, the VCN–DCN array consists of five 32-site four-shank probes secured in a mounting platform to form a 160-site device. Two probe designs were developed: one for VCN and the other for DCN; specifications are listed in Table I. Both designs had a maximum shank width of 61 μm in order to minimize any disruption to the neural circuitry during implantation. This was achieved by using an interconnect line width of 2 μm when necessary. The shanks also taper in the region, where the sites are located to keep the width at a minimum as the interconnect lines reach their designated endpoints.

1) Ventral Cochlear Nucleus Probes: Three of the five probes in the array are targeted at VCN. The VCN probe design has four shanks at a pitch of 200 μm, as shown in Fig. 2. The total length from the bottom of the platform to the center of the tip-most site is 5 mm. The merged shank region at the base of the array remains outside the cerebellum after implantation and spans the distance to the platform required by the insertion angle and insertion depth. By merging this region, the strength of the probe was increased; the impedances of the interconnect lines were also decreased since their line widths could be increased there.

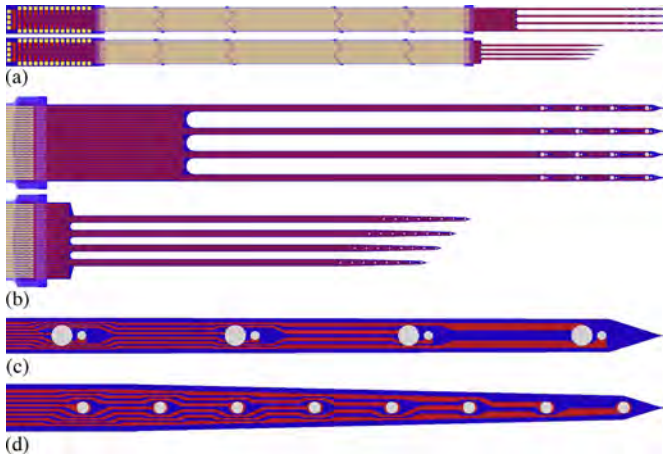

Fig. 2. Device layouts showing the (a) integrated polymer cables for interfacing with (b) VCN and DCN probes as well as close-ups of (c) VCN stimulation and recording site pairs and (d) DCN sites.

Recording and stimulation offer conflicting constraints on electrode site area. Although single units may be more easily isolated with smaller sites, the maximum safe stimulating current levels would be substantially less with smaller area higher impedance sites. In order to both record and stimulate effectively with the VCN probe, the sites were arranged in pairs. The smaller site of each pair was designated for recording and had a site area of 177 μm^2. The larger site of each pair had an area of 1000 μm^2 and was intended for stimulation. There are four-site pairs per shank at a pitch of 300 μm for a total of eight sites per shank and thirty-two sites per probe. The site designations for recording and stimulation are purely based on site area; beside the aforementioned discussion, any of the sites are suitable for recording or stimulation.

2) Dorsal Cochlear Nucleus Probes: The remaining two probes were designated for the DCN, with four shanks at a pitch of 125 μm, as illustrated in Fig. 2. The desired recording locations in the DCN are within the top layers, up to a few hundred micrometers deep. Since the surface of the DCN is dome shaped, the shanks were designed with staggered lengths to account for the surface curvature and maintain recordings within the top layers across a given mediolateral probe position. The length of the lateral-most shank from the bottom of the platform to the center of the tip-most site is 3400 μm; subsequent shanks each decrease in length by 125 μm. There are eight equally spaced sites per shank at a pitch of 100 μm. All of the sites have an area of 177 μm^2; although this site size is more appropriate for recording, these sites may also be used for stimulation.

C. 3-D Structure and Block Platform

The 3-D microassembly of boron-doped silicon probes has been previously achieved using a thin platform through which 2-D probes were placed and secured with spacers [10]–[13].

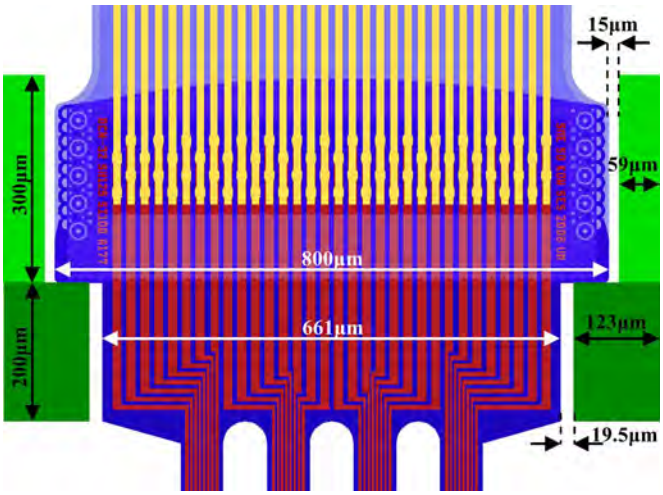

Fig. 3. Cross-sectional drawing of a probe in a platform slot.

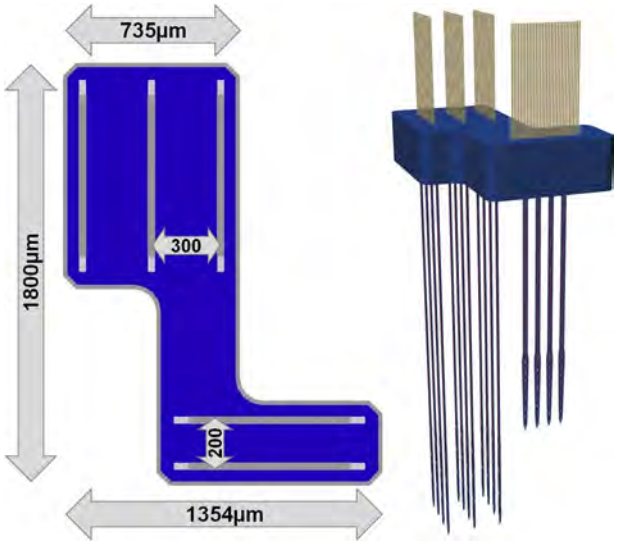

Fig. 4. Platform layout and conceptual drawing of the 3-D array.

However, for large numbers of leads, this approach results in substantial wings on the ends of the probes, where the probe-platform lead transfers are made, increasing the size of the implant. More recently, an improved structure has been developed, in which the probes are inserted in slots formed using deep reactive ion etching (DRIE) in a platform formed from full-thickness (500 μm) 4-in silicon wafers [14]. The probes are held parallel by designing the vertical slots only slightly larger than the probes themselves, eliminating the need for any wings or platform spacers. A parylene overlay cable is bonded to the lead tabs coming from the probes [14], taking the neural signals to an adjacent signal-processing chip or directly to the external setup. The low profile of this design is especially important in chronic applications, minimizing overall implant size, and allowing the dura to be replaced over it. However, for acute applications, such as neural mapping, the structure can be further simplified by integrating the output cables directly into the probes themselves, completely eliminating any bonds or lead transfers at the implant site.

This paper employs a slotted 500-μm-thick platform with probes containing 10-mm-long integrated parylene cables. The cables route the leads from the back ends of the probes embedded in the platform out of the surgical access hole. The five cables from the probes may be stacked to form a space-saving "multilevel" interconnect, which is important for high-density designs, as in this paper. Each cable is less than three-fourths of a millimeter wide at its widest point, carrying 32 interconnect lines at a 20-μm pitch. Platform size constraints prevent expanding the platform to fit wider leads.

The platform slots mechanically secure the individual probes. Top (300-μm deep) and bottom (200-μm deep) DRIE etches form the slots and the overall platform shape. The top slot is longer than the bottom slot so that a ledge is formed, on which the probe rests when fully inserted, as illustrated in Fig. 3. The back ends of the VCN and DCN probes both employ this same design for countersinking them into the platform. The width of the platform slots is based on the fabrication thicknesses of the various probe layers. The top portion of the probe back end is 25-μm thick; the top slots are 29-μm thick, resulting in a 4-μm tolerance. The bottom slot width extends past the top by 1 μm on each side.

Several constraints determined the platform footprint for the VCN–DCN arrays. The exposed area for viewing and probe placement is extremely limited for the surgical and experimental reasons previously described. Therefore, the mediolateral and rostrocaudal dimensions of the platform must be not larger than necessary to support the probes. The narrow platform design, with a 1.18-mm^2 footprint, suspends probes with slots only 50 μm from the edge of the platform in one direction and 59 μm in the other. Since the AVCN is farther lateral than the DCN, the VCN probe slots are offset to the left of center in relation to the DCN slots, as presented in Fig. 4. Table II lists the platform specifications. The VCN probe slot pitch is 300 μm and the DCN probe slot pitch is 200 μm. The distance between the closest DCN and VCN probe slots is 628 μm. The VCN and DCN platform slots are perpendicular to each other in order to span the tonotopically organized subdivisions of the CN. The notched shape of the platform offers a reduced footprint over a rectangular design, allowing greater visibility of the probe shanks during surgical implantation and a lower weight for a chronic prosthesis. The 3-D 160-site array is also illustrated conceptually in Fig. 4.

III. Fabrication and Assembly

The 2-D probe process flow was based on the well-established passive-probe technology developed at the University of Michigan, which employs boron etch-stops to enable thin ($\sim$12-μm substrate) devices to be batch fabricated with integrated polymer cables [13], [15]. Table III lists the major process steps and layer thicknesses for the 2-D probes. The block platforms were fabricated using DRIE following a process similar to [14]. A photograph of fabricated devices is shown in Fig. 5.

A custom micromachined jig was used to hold the platform during assembly. In this 500-μm-thick frame, 250-μm-deep

TABLE II
PLATFORM SPECIFICATIONS FOR THE VCN–DCN 3-D ARRAY

	VCN Area	DCN Area
Length (rostro-caudal)	947μm	335μm
Width (medio-lateral)	735μm	948μm
Max Probes per Array	3	2
Probe Pitch	300μm	200μm
	Overall	
Total Length	1800μm	
Total Width	1354μm	
Thickness (dorso-ventral)	500μm	
	Top (Major)	Bottom (Minor)
Slot Thickness	29μm	31μm
Slot Width	830μm	700μm
Slot Depth	300μm	200μm
Rim Etch	16μm	17μm

TABLE III
PROBE FABRICATION STEPS AND TARGET PARAMETERS

Material	Thickness	Method
Deep & Shallow Boron Substrate	12μm	Diffusion
Pad Oxide	1500Å	Thermal
Oxide/Nitride/Oxide	3000Å/1500Å/3000Å	LPCVD[a]
Doped Polysilicon Leads	6000Å	LPCVD / Etch
Pad Oxide	1500Å	Thermal
Oxide/Nitride	3000Å/1500Å	LPCVD
Large Contact	--	RIE[b]
Oxide	3000Å	LPCVD
Small Contact	--	RIE
Titanium (Ti)/Iridium Sites (Ir)	500Å/3000Å	Sputtered / Liftoff
Chromium (Cr)/Gold Pads (Au)	500Å/300Å	Sputtered / Liftoff
Dielectric Etch	--	RIE
Bottom Parylene	2μm	Deposition / Etch
Chromium (Cr) /Gold Leads (Au)	250Å/1000Å	Sputtered / Liftoff
Silicon Anchor	--	DRIE[c]
Top Parylene	3μm	Deposition / Etch
Thinning	--	DRIE
Release	--	TMAH[d]
Totals	Thickness	Steps
Back-end Top	24.875μm	All except 6
Back-end Bottom & Shanks	14.75μm	Through step 8

[a]Low-Presure Chemical Vapor Deposition
[b]Reactive Ion Etching
[c]Deep Reactive Ion Etching
[d]Tetramethylammonium Hydroxide

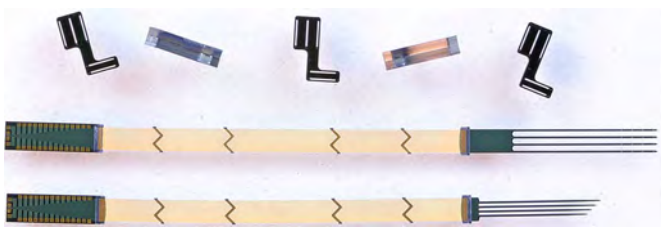

Fig. 5. Photograph of fabricated probes and platforms. Five platforms are shown; two are standing on their edge.

recesses were etched by DRIE for multiple platforms to enable the assembly of several arrays at once. The probes were positioned in the platform slots with a vacuum wand attached to a micromanipulator. A small amount of medical grade silicone (Med-4211, NuSil Technology LLC) was used to secure the probes in place and to seal the top and bottom ends of the platform slots.

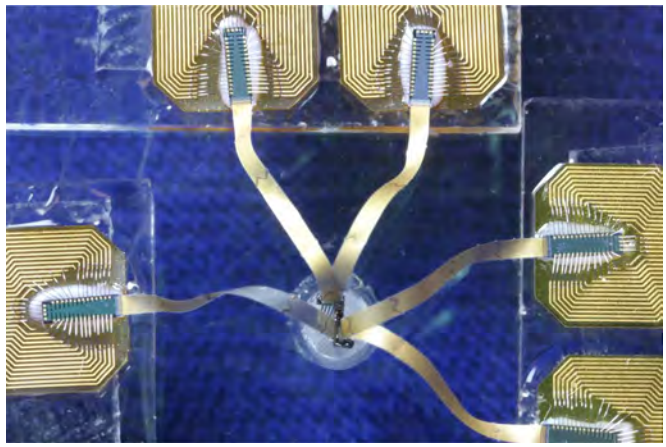

Fig. 6. Photograph of a five-probe array in the Plexiglas workholder after wire bonding between the integrated parylene cables and hybrid polyimide cables.

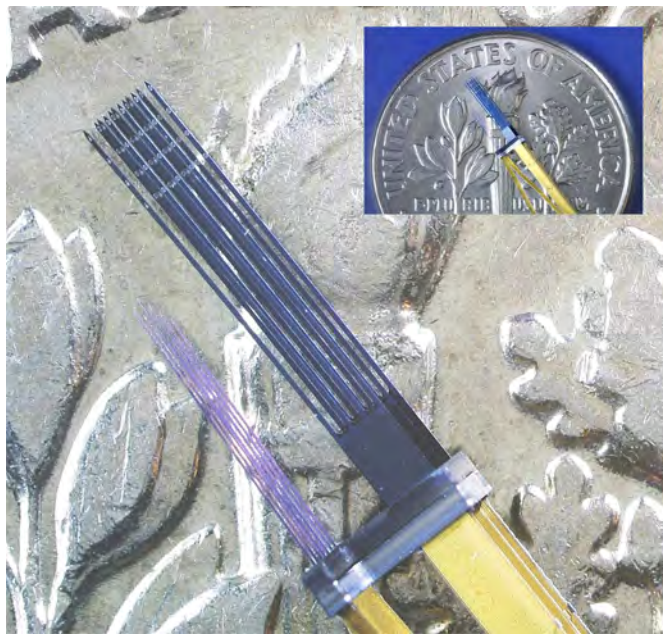

Fig. 7. Photograph of a 160-site 3-D VCN–DCN mapping array on the back of a U.S. dime.

The parylene cables terminate in an integrated silicon bonding region. Ultrasonic wire bonding was used to connect them to flexible 25-cm-long polyimide printed circuit board (PCB) cables (manufactured by SunTech Circuits, Inc.), which attach to a site-selection board. A custom Plexiglas work holder, shown in Fig. 6, restrained the array to enable bonding between the integrated parylene and hybrid polyimide cables. Fig. 7 shows an assembled five-probe array.

IV. *In Vivo* RESULTS

A. *Surgical Approach and Verification of Probe Placement*

The typical surgical preparation followed that of previously reported work with other electrodes [16]. The work was in accord with the National Institutes of Health (NIH) Guidelines for the Use and Care of Laboratory Animals (NIH publication

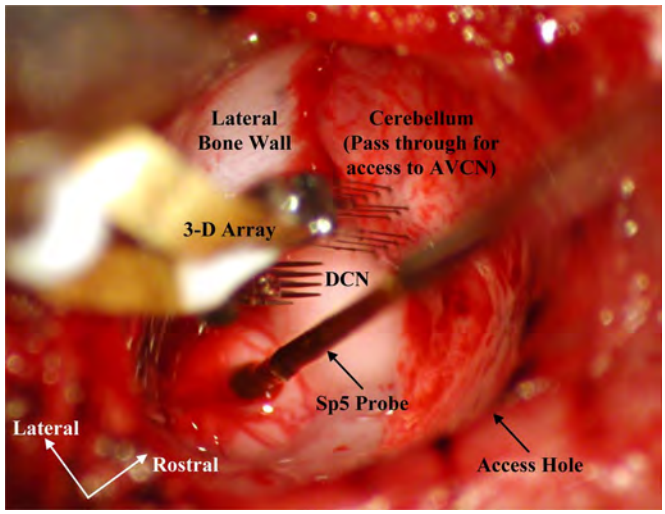

Fig. 8. Photograph of a five-probe array implanted in the CN of a guinea pig.

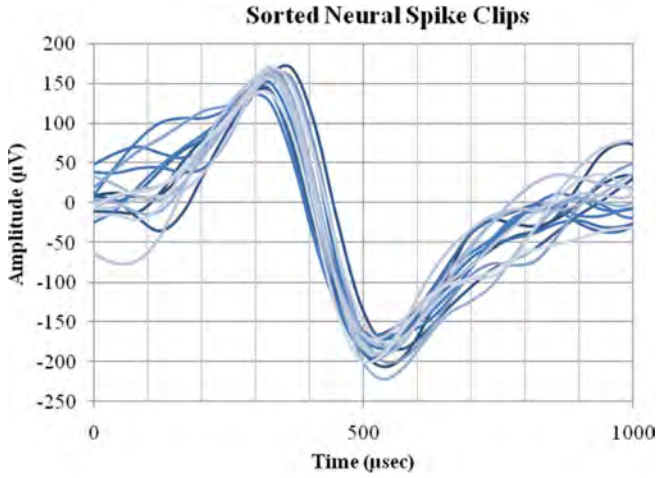

Fig. 9. *In vivo* recordings of neural waveforms [8].

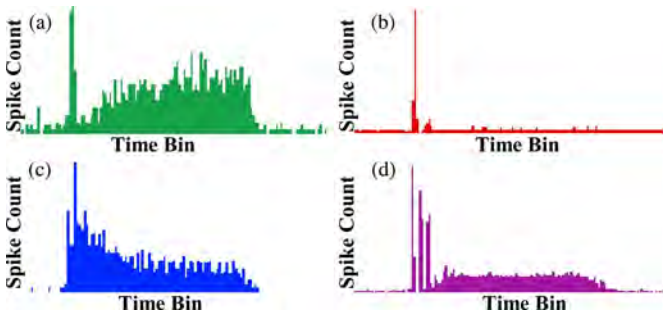

Fig. 10. PSTHs from *in vivo* recordings of neural activity showing (a) pauser buildup, (b) onset, (c) primary like, and (d) chopper response patterns.

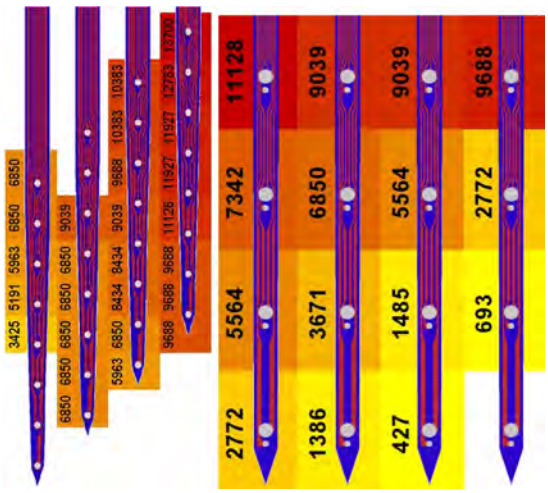

Fig. 11. Frequency map of a (left) DCN and (right) a VCN probe. The per channel CF was determined using ten repetitions of a 50-ms acoustic tone for each stimulus condition set (frequency/sound level).

No. 80–23) as well as with the guidelines by the University of Michigan Committee on the Use and Care of Animals. Pigmented guinea pigs from Cady Ridge Farms (Chelmsford, MA, USA) of young adult size/age (300–800 g) were anesthetized using ketamine (40 mg/kg) and xylazine (10 mg/kg). A stereotactic frame stabilized the subject during surgery and recording, which took place in an electrically shielded and double-walled sound booth. The surgery included a craniotomy and partial aspiration of the cerebellum overlying the DCN. Hollow earbars joined to speakers (Beyer DT770pro) provided the acoustic stimulus.

The VCN–DCN 3-D array was stereotactically implanted, as shown in Fig. 8. The location of the array in the tissue was marked by dipping the shanks in FG dye prior to insertion and with an electrolytic lesion at the end of the experiment. Placement of electrode sites in DCN and AVCN were confirmed in serial brain sections. Animal ground was defined by connecting the neck muscles to the ground and reference pins of the head stage (RA16AC, Tucker Davis Technologies).

B. Single and Multiunit Recordings

The primary purpose of the VCN–DCN array is to simultaneously record from both CN subdivisions. This was achieved repeatedly during *in vivo* experiments. Fig. 9 presents the clips of neural spikes for one of the recorded units. The complexity of the CN is underscored by its diverse cytoarchitecture. Over ten cell types are grouped in part by location [9]; the peri-stimulus time histogram (PSTH) of a CN neuron is one indicator of cell type. A spread of response patterns has been observed from recordings with the VCN–DCN array; a selection of these responses is presented in Fig. 10 for both subnuclei.

C. Tonotopic Mapping

It is well known that the CN is tonotopically organized, representing a spatial array of all frequencies that are coded by the incoming auditory nerve. This tonotopic pattern is repeated within each subdivision. In some experiments, such as those investigating aspects required for auditory prostheses, it is desirable to simultaneously record (or stimulate) from neurons with similar characteristic frequencies (CFs) in both subnuclei. The high-density 3-D array enables one to plot the CFs with respect to instrumented location. The recorded frequency map aids the researcher in intuitively visualizing corresponding CFs and their anatomical location. Fig. 11 shows recorded CF maps for two probes.

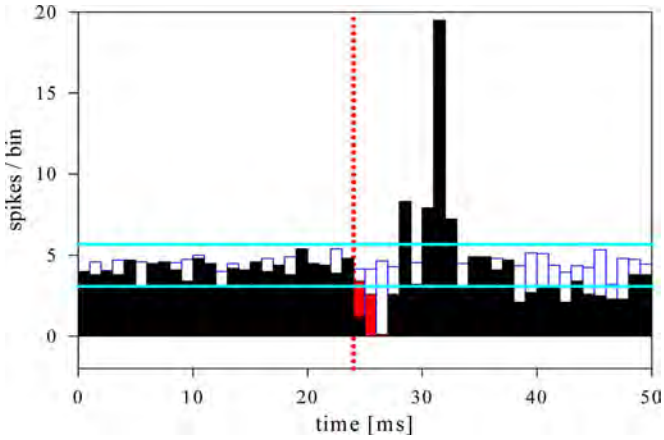

Fig. 12. PSTH of elicited neural activity in DCN due to electrical stimulation in VCN. The blue-outlined bars indicate spontaneous rate (measured after the stimulus period). The horizontal aqua lines designate 2.86 standard deviations from the average spontaneous rate. The red bars are the sorted stimulus artifacts and the black bars are the sorted spikes during the stimulus time frame. Dotted red line indicates stimulus onset.

D. Intersubnuclei Mapping

The neural architecture is composed of complex circuits and subcircuits. Electrical stimulation, as a complementary approach to anterograde and retrograde tracing studies, enables the study of the living network from the perspective of particular connections. Previous studies have investigated intrinsic pathways within the CN [17]–[21]. To expand on this understanding, in this paper, the bimodal (stimulate/record) approach was used to explore the connections between the AVCN and DCN. The stimulus configuration consisted of 50 pulse trains at 20 Hz of 10 current pulses each. The pulses were charge balanced, biphasic, negative first, and of 10-μA amplitude. Fig. 12 shows elicited responses of a selected DCN channel before and during electrical stimulation on one channel in VCN; the response pattern shows a decrease in spike count immediately after the stimulus followed by significant excitation and then further inhibition. While further experiments are necessary before conclusions can be made about the connectivity between VCN and DCN channels, the *in vivo* work to date demonstrates the value of high-density electrode arrays tailored to specific anatomical structures and in particular the 160-site 3-D VCN–DCN array developed here for studying the underlying neural circuits.

V. Conclusion

The device presented in this paper represents one of the most advanced high-density neural interfaces ever reported and is the first 3-D array with over 100 sites for mapping in the guinea pig VCN–DCN. The VCN–DCN array has not only been used during *in vivo* experimentation, which proved its functionality, but it has also contributed to neuroscience research enabling studies not heretofore feasible. Experiments exploring auditory-somatosensory integration continue to use this device; the application-specific design permits high-density recording in two CN subnuclei with a commercial stimulation probe in the spinal trigeminal nucleus. On-going studies will focus on the intrinsic connections between the VCN and DCN subregions using bimodal functionality to simultaneously stimulate electrically and record the elicited waveforms. Additional experiments are also being planned using this array as a prototype for an auditory prosthesis. This application-specific device is not only a high-density interface for the guinea pig CN, but also stands as the forerunner for future silicon-based electrode arrays, which focus on target-specific neuroscience and medical needs, including neural mapping and prosthetic system prototypes.

Acknowledgment

The authors would like to thank Mr. B. Casey (bonding and packaging), Ms. M. N. Gulari (layout and fabrication guidance), Sister M. R. Villareal (impedance testing), Sister M. J. Campbell (workholder machining), Mr. C. Yun (site selection board design), Mr. C. Ellinger and Mr. D. Vailliencourt (setup support), and Mr. S. Koehler (software support). The authors would also like to acknowledge the contributions of the University of Michigan Lurie Nanofabrication Facility in enabling the electrode fabrication.

References

[1] R. A. Normann, "Technology insight: Future neuroprosthetic therapies for disorders of the nervous system," *Nat. Clin. Pract. Neurol.*, vol. 3, pp. 444–452, Aug. 2007.
[2] J. C. Middlebrooks and R. L. Snyder, "Intraneural stimulation for auditory prosthesis: Modiolar trunk and intracranial stimulation sites," *Hear. Res.*, vol. 242, pp. 52–63, Aug. 2008.
[3] D. McCreery, A. Lossinsky, and V. Pikov, "Performance of multisite silicon microprobes implanted chronically in the ventral cochlear nucleus of the cat," *IEEE Trans. Biomed. Eng.*, vol. 54, pp. 1042–1052, Jun. 2007.
[4] D. B. McCreery, "Cochlear nucleus auditory prostheses," *Hear. Res.*, vol. 242, pp. 64–73, Aug. 2008.
[5] H. H. Lim, T. Lenarz, D. J. Anderson, and M. Lenarz, "The auditory midbrain implant: Effects of electrode location," *Hear. Res.*, vol. 242, pp. 74–85, Aug. 2008.
[6] D. J. Anderson, "Penetrating multichannel stimulation and recording electrodes in auditory prosthesis research," *Hear. Res.*, vol. 242, pp. 31–41, Aug. 2008.
[7] Sister M. E. Merriam, "A three-dimensional bidirectional interface for neural mapping studies," Ph.D. dissertation, Dept. of Elect. Eng., Univ. of Michigan, Ann Arbor, MI, 2010.
[8] M. E. Merriam, S. Dehmel, O. Srivannavit, S. E. Shore, and K. D. Wise, "Three-dimensional 160-site microelectrode array for cochlear nucleus mapping studies," in *Proc. Ann. Fall Meet. Biomed. Eng. Soc.*, Austin, TX, Oct. 2010.
[9] C. M. Hackney, K. K. Osen, and J. Kolston, "Anatomy of the cochlear nuclear complex of guinea pig," *Anat. Embryol.*, vol. 182, pp. 123–149, 1990.
[10] A. C. Hoogerwerf and K. D. Wise, "A three-dimensional microelectrode array for chronic neural recording," *IEEE Trans. Biomed. Eng.*, vol. 41, pp. 1136–1146, Dec. 1994.
[11] Q. Bai, K. D. Wise, and D. J. Anderson, "A high-yield microassembly structure for three-dimensional microelectrode arrays," *IEEE Trans. Biomed. Eng.*, vol. 47, pp. 28–289, Mar. 2000.
[12] M. D. Gingerich, J. F. Hetke, D. J. Anderson, and K. D. Wise, "A 256-site 3D CMOS microelectrode array for multipoint stimulation and recording in the central nervous system," presented at the Int. Conf. on Solid-State Sensors and Actuators (Transducers), Munich, Germany, Jun. 2001.
[13] Y. Yao, M. N. Gulari, J. A. Wiler, and K. D. Wise, "A microassembled low-profile three-dimensional microelectrode array for neural prosthesis applications," *J. Microelectromech. Syst.*, vol. 16, pp. 977–988, Aug. 2007.
[14] G. E. Perlin and K. D. Wise, "A compact architecture for three-dimensional neural microelectrode arrays," in *Proc. 30th Annu. Int. IEEE Conf. Eng. Med. Biol. Soc. (EMBS)*, Vancouver, Canada, 2008, pp. 5806–5809.

[15] Y. Yao, M. N. Gulari, B. Casey, J. A. Wiler, and K. D. Wise, "Silicon microelectrodes with flexible integrated cables for neural implant applications," in *Proc. 3rd Int. IEEE Eng. Med. Biol. Soc. (EMBS) Conf. Neural Engineering*, Kohala Coast, HI, 2007, pp. 398–401.
[16] S. E. Shore, S. Koehler, M. Oldakowski, L. F. Hughes, and S. Syed, "Dorsal cochlear nucleus responses to somatosensory stimulation are enhanced after noise-induced hearing loss," *Eur. J. Neurosci.*, vol. 27, pp. 155–168, Jan. 2008.
[17] E. F. Evans and P. G. Nelson, "On the functional relationship between the dorsal and ventral divisions of the cochlear nucleus of the cat," *Exp. Brain Res.*, vol. 17, pp. 428–442, Jun. 1973.
[18] W. P. Shofner and E. D. Young, "Inhibitory connections between AVCN and DCN: Evidence from lidocaine injection in AVCN," *Hear. Res.*, vol. 29, pp. 45–53, 1987.
[19] P. X. Joris and P. H. Smith, "Temporal and binaural properties in dorsal cochlear nucleus and its output tract," *J. Neurosci.*, vol. 18, pp. 10157–10170, Dec. 1998.
[20] R. H. Arnott, M. N. Wallace, T. M. Shackleton, and A. R. Palmer, "Onset neurones in the anteroventral cochlear nucleus project to the dorsal cochlear nucleus," *J. Assoc. Res. Otolaryngol.*, vol. 5, pp. 153–170, Jun. 2004.
[21] J. R. Doucet and D. K. Ryugo, "Structural and functional classes of multipolar cells in the ventral cochlear nucleus," *Anat. Rec. A Discov. Mol. Cell. Evol. Biol.*, vol. 288, no. 4, pp. 331–344, Apr. 2006.

Sister Mary Elizabeth Merriam received the B.S. degree from Rensselaer Polytechnic Institute, Troy, NY, in 1999, and the M.S. and Ph.D. degrees from the University of Michigan, Ann Arbor, in 2001 and 2010, respectively, all in electrical engineering.

During her undergraduate years, she was an Intern at Eastman Kodak Company. In 2002, she entered the Dominican Sisters of Mary, Mother of the Eucharist. From 2000 to 2002 and 2007 to 2010, she was a Research Assistant at the Center for Wireless Integrated MicroSystems. She is currently a Teacher at St. Dominic Savio Catholic High School, Austin, TX. Her research interest include electrode arrays for neural interfaces.

Susanne Dehmel received the Dipl. degree in biology and the Ph.D. degree from the University of Leipzig, Germany in 1999 and 2006, respectively.

Since 2007, she has been a Postdoctoral Fellow at the Kresge Hearing Research Institute, Department of Otolaryngology, University of Michigan. Her research interests include signal processing in the normal and pathological auditory system.

Onnop Srivannavit received the B.S. degree in chemical technology and the M.S. degree in petrochemical technology from Chulalongkorn University, Pathumwan, Thailand, and the Ph.D. degree in chemical engineering from the University of Michigan, Ann Arbor, in 2002.

He is currently a Research Engineer at the University of Michigan. His research interest includes the development of microelectromechanical systems and microfluidic devices for biomedical and environmental applications.

Susan E. Shore received the M.A. (cum laude) degree in auditory science from the University of Witwatersrand, Johannesburg, South Africa, in 1976, and the Ph.D. in physiology from the Kresge Hearing Research Laboratory, Department of Otolaryngology, University of Michigan, Ann Arbor, and the Deparment of Physiology, Louisiana State Medical School, New Orleans, in 1981.

He was a Postdoctoral Fellow at the University of Pittsburgh, Pittsburgh, PA, and the University of Michigan. She is currently an Associate Professor in the Department of Molecular and Integrative Physiology, and a Research Professor in the Department of Otolaryngology, University of Michigan.

Sr. Shore was the recipient of the Research Faculty Achievement Award at the University of Michigan in 2006.

Kensall D. Wise received the B.S.E.E. degree (with distinction) from Purdue University, West Lafayette, IN, in 1963, and the MS and Ph.D. degrees in electrical engineering from Stanford University, Palo Alto, CA, in 1964 and 1969, respectively.

From 1963 to 1965 and from 1972 to 1974, he was a member of the Technical Staff at Bell Telephone Laboratories, where his study focused on the exploratory development of integrated electronics for use in telephone communications. From 1965 to 1972, he was a Research Assistant and then a Research Associate and Lecturer at the Department of Electrical Engineering, Stanford University, where he was engaged in the development of micromachined solid-state sensors. In 1974, he joined the Department of Electrical Engineering and Computer Science, University of Michigan, Ann Arbor, where he is now the J. Reid and Polly Anderson Professor of Manufacturing Technology, Director of the Engineering Research Center for Wireless Integrated MicroSystems, and Director of the Lurie Nanofabrication Facility. His current research includes the development of integrated microsystems for health care, environmental monitoring, and defense applications.

Dr. Wise organized and was as the first chairman of the Technical Subcommittee on Solid-State Sensors of the IEEE Electron Devices Society (EDS). He was the General Chairman of the 1984 IEEE Solid-State Sensor Conference, was an IEEE-EDS National Lecturer (1986), and was he Technical Program Chairman (1985) and General Chairman (1997) of the IEEE International Conference on Solid-State Sensors, Actuators, and Microsystems. He was the recipient of the Paul Rappaport Award from the EDS (1990), a Distinguished Faculty Achievement Award from the University of Michigan (1995), the Columbus Prize from the Christopher Columbus Fellowship Foundation (1996), the SRC Aristotle Award (1997), and the 1999 IEEE Solid-State Circuits Field Award. In 2002, he was named the William Gould Dow Distinguished University Professor at the University of Michigan. He held the 2007 Henry Russel Lectureship at the University and is a Fellow of the American Institute of Medical and Biological Engineering, and a member of the United States National Academy of Engineering.